Applied Catalysis B: Environmental 147 (2014) 35–42

Applied Catalysis B: Environmental

journal homepage: www.elsevier.com/locate/apcatb

Effects of nitrogen compounds, aromatics, and aprotic solvents on the oxidative desulfurization (ODS) of light cycle oil over Ti-SBA-15 catalyst

Kye-Sung Cho, Yong-Kul Lee*

Laboratory of Advanced Catalysis for Energy and Environment, Department of Chemical Engineering, Dankook University, 126 Jukjeondong, Yongin 448-701, South Korea

ARTICLE INFO

Article history:
Received 23 May 2013
Received in revised form 24 July 2013
Accepted 8 August 2013
Available online 29 August 2013

Keywords:
Oxidative desulfurization
Light cycle oil
4,6-DMDBT
Ti-SBA-15
Aprotic solvent

ABSTRACT

Effects of nitrogen compounds, aromatics, and aprotic solvents on the oxidative desulfurization (ODS) of refractory sulfur compounds and light cycle oil over Ti-SBA-15 catalyst were studied in a batch or a continuous fixed-bed reactor with tert-butyl hydroperoxide (TBHP) as oxidant. The fresh and spent catalysts were characterized by BET, TGA, ICP-AES, and X-ray absorption spectroscopy. The nitrogen compounds were found to inhibit the ODS in the order: indole > quinoline > carbazole. The addition of aromatics solvent in feed gradually recovered the ODS activity for LCO. Moreover, the aprotic solvent significantly promoted the LCO ODS. These results were attributed to the high solubility of the oxidized S or N compounds in the aromatics and aprotic solvents, minimizing the deposit of oxidized product on the surface of the catalyst.

1. Introduction

The operation of residual fluid catalytic cracker (RFCC) and fluid catalytic cracker (FCC) is essential process to meet the increasing demand of light oil and transportation fuel. The light cycle oil (LCO), a by-product of these processes, is known as a poor diesel fuel blending component due to its poor engine ignition performance and high sulfur, nitrogen and aromatic contents. Considering the high contents of hetero-cyclic compounds in LCO, the conventional hydrotreating catalysts may suffer from the competition reactivity of hydrodesulfurization (HDS), hydrodenitrogenation (HDN), hydrogenation of aromatics (HDA), and hydrocracking (HCK) [1–6]. Sulfur compounds in LCO are present in the alkyl derivatives of dibenzothiophene, especially dimethyldibenzothiophene (C2-DBT). These compounds are poor in HDS reactivity and are classified as the most refractory compounds in conventional HDS process as they cause steric hindrance [7–9]. Reactivity of the alkyl-dibenzothiophenes decreases in the presence of inhibitors like polyaromatics and nitrogen compounds, normally found in the LCO feed. Thus, the operation conditions result in large hydrogen consumption, reduction of the catalyst life, and significant increase of the operation cost [10]. This tends to limit the application of the hydrotreatment for the desulfurization of LCO. The alternative technologies have thus been introduced to overcome the present limitation of desulfurization technique. Biodesulfurization, adsorption, ionic liquids extraction, and oxidative desulfurization (ODS) were introduced to achieve ultra-low sulfur diesel [11–18]. Among them the ODS has been considered to be one of the most promising methods for ultra-deep desulfurization of fuel oil due to its several advantages over HDS: (i) mild reaction conditions at low temperature (<100 °C) and under atmospheric pressure; (ii) no use of the expensive hydrogen; (iii) higher reactivity of aromatic sulfur species.

In the ODS process, the refractory sulfur compounds are oxidized into their corresponding sulfones or sulfoxides, and these are subsequently removed by extraction, absorption, distillation, or decomposition [19–24]. Ishihara et al. [20], Prasad et al. [25], and G-Gutierrez et al. [26] have shown that molybdenum oxide catalysts have shown activity in ODS of the refractory sulfur compounds. However, molybdenum oxide catalysts are known to have critical drawbacks of Mo-leaching in the course of ODS. In contrast, Chica et al. [27] reported that Ti-MCM-41 catalyst was more active and stable in ODS than MoO_3/Al_2O_3 catalysts without Ti-leaching. Hulea et al. [23] and Corma et al. [28] found that Ti-MCM-41 was more active than TS-1, proving that the accessibility of the S compounds to the active centers is important in ODS of refractory S compounds. Cedeno-Caero et al. [29] reported that titanium oxide nanotube catalyst was more active in ODS than TiO_2 catalysts. More recently, Ti-SBA-15 catalysts were reported to exhibit high activity in the ODS [30]. Although much research has been made in the

* Corresponding author. Tel.: +82 3180053466.
E-mail address: yolee@dankook.ac.kr (Y.-K. Lee).

0926-3373/$ – see front matter © 2013 Elsevier B.V. All rights reserved.
http://dx.doi.org/10.1016/j.apcatb.2013.08.017

Table 1
Specifications of light cycle oil (LCO).

Physical properties	LCO
API	13.5
S (ppm)	3600
N (ppm)	550
Color (ASTM)	L2.5
Aromatics (wt%)	
Total	74.3
Mono	14.3
Di	40.6
Tri+	19.4
Cetane Index	24.9
Distillation (°C)	
IBP/5/10/	225/256/262/
30/40/50/	284/292/308/
60/90/95/	325/398/–/
EP	–

Table 2
Composition of model feed oils.

Model feeds		Notation
Benzothiophene (BT)	200 ppm S	Feed-M
Dibenzothiophene (DBT)	200 ppm S	
4-Methyldibenzothiophene (4-MDBT)	200 ppm S	
4,6-Dimethyldibenzothiophene (4,6-DMDBT)	200 ppm S	
Tridecane	Balance	
Feed-M + tetralin (1Ar)	800 ppm S	-M1A
Feed-M + 1-methylnaphthalene (2Ar)	800 ppm S	-M2A
Feed-M + indole	800 ppm S, 50 ppm N	-MI
Feed-M + quinoline	800 ppm S, 50 ppm N	-MQ
Feed-M + carbazole	800 ppm S, 50 ppm N	-MC
Feed-M + tetralin + indole	800 ppm S, 50 ppm N	-M1AI
Feed-M + 1-methylnaphthalene + indole	800 ppm S, 50 ppm N	-M2AI
Feed-M + acetonitrile + indole	800 ppm S, 50 ppm N	-MAcI

ODS of refractory sulfur compounds, few studies were introduced to examine the effect of aromatics and nitrogen compounds which are commonly found in the real feed oils [24].

In this study, the ODS of model sulfur compounds and real LCO feed on the Ti-SBA-15 catalyst was studied in either a batch or a continuous fixed-bed reactor with TBHP as oxidant. In particular, effects of various nitrogen compounds, aromatics, and aprotic solvents on the ODS activity and stability were also investigated.

2. Experimental

2.1. Materials and catalysts preparation

Model compounds and chemicals, including benzothiophene (BT, Aldrich, 99%), dibenzothiophene (DBT, Aldrich, 98%), 4-methyldibenzothiophene (4M-DBT, Aldrich, 96%), 4,6-dimethyldibenzothiophene (4,6-DMDBT, Aldrich, 97%), dibenzothiophene sulfone (DBTS, Aldrich, 97%), indole (Aldrich, 99%), carbazole (Aldrich, 95%), quinoline (Aldrich, 98%), oxindole (Alfa Aesar, 97%), 5.0–6.0 M TBHP in decane (Aldrich), n-tridecane (TCI, 99%), tetralin (Aldrich, 97%) and 1-methylanaphthalene (Alfa Aesar, 98%) were used as received. The LCO feed was supplied from a refinery in Korea and the specification is given in Table 1.

SBA-15 was hydrothermally synthesized according to the procedures reported previously [31]. Pluronic P123 [poly(ethylene glycol)-block-poly(propylene glycol)-block-poly(ethylene glycol), Aldrich] of tri-block copolymer was dissolved in 1.6 M HCl solution with stirring and then the silica source of tetraethyl orthosilicate (TEOS, Aldrich) was added in the tri-block copolymer solution with stirring for 1 h at 308 K. The mixture was reacted for 20 h at 308 K and subsequently hydrothermally treated for 24 h at 353 K. The precipitates were filtered, washed with distilled water, dried overnight in an oven at 373 K, and then calcined in air at 773 K for 6 h.

Grafting method was used to prepare Ti-SBA-15 catalyst with tetra butyl orthotitanate (TBOT, Aldrich) as a Ti source [36]. In a typical preparation, 0.35 g of TBOT was hydrolyzed in 20 g of glycerol to obtain a homogeneous solution. To the solution was added 1 g of SBA-15, and then the mixture was heated at 373 K for 70 h. After the grafting procedure, the Ti-grafted SBA-15 sample was filtered, washed with deionized water, and calcined at 823 K for 4 h.

2.2. Catalyst characterization

A Micromeritics ASAP 2010 micropore size analyzer was used to measure the specific surface area of the sample from the linear portion of BET plots (P/Po = 0.01–0.10) at 77 K. The Ti K-edge (4.965 keV) X-ray absorption (XAS) spectra of catalyst samples were recorded in the energy range 4.915–5.065 keV using a synchrotron radiation at the beamlines 8 C and 10 C, Pohang Light Source (PLS). The X-ray ring at the PLS has a flux of 1×10^{10} photons s^{-1} at 100 mA and 2.5 GeV. The X-ray beamline is equipped with a Si (1 1 1) channel-cut monochrometor and has an energy range capability of 4–33 keV. The amount of chemical deposits on the catalysts after the ODS tests was quantified by TGA (SDT2960, TA instruments). The metal content of the catalyst samples was determined by inductively coupled plasma-atomic emission spectroscopy (ICP-AES, Perkin Elmer, Model Optima-4300 DV).

2.3. Solubility measurements

The excess amount of oxidized model compounds of DBTS, indole and isatin was dissolved in tridecane (10 ml) at 293 K. After the mixture was stirred for 1 h, it was separated by centrifugation. The upper solution was analyzed by GC-FID (Agilent-6890, DB-1) to calculate solubilities of the oxidized model compounds. The solubility was also measured for tetralin, 1-methylnaphtalene, and acetonitrile.

2.4. Activity test

The specifications of model feed mixture used in this study are summarized in Table 2. The ODS was carried out at atmosphere and 80 °C in a 100 ml glass batch reactor equipped with a temperature controller, a condenser, and mechanical stirrer using a model feed mixture containing sulfur compounds. Also, model ODN tests were employed to confirm the competitive oxidation behaviors using indole, carbazole, and quinoline, known as the most typical nitrogen compounds in LCO [37]. Typically, 50 g of feed containing the model sulfur and nitrogen compounds with a molar ratio of TBHP/(S + N) of 2.5 was combined by 0.12 g of catalyst and the ODS was carried out for 1 h at 80 °C. For LCO feed containing 3700 ppm S, the ODS activity of test was carried out in the batch reactor or a continuous fixed-bed reactor. In a typical run, 30 g of LCO feed with TBHP in decane (TBHP/S ratio = 2.5) was heated to 80 °C, then 1 g of catalyst were added in the batch reactor. The ODS of LCO feed was then performed in a fixed-bed stainless-steel reactor. 1 g (1.5 ml) of catalyst sample was packed at the center of a stainless steel reactor (300 mm long and 8 mm i.d.). The LCO feed pre-mixed with the oxidizing agent (TBHP/S ratio = 2.5) was fed into a preheated reactor. The oxidation reaction was conducted at 80 °C with a WHSV = 2 h^{-1} operating at atmospheric pressure. The reaction progress was monitored by collecting the product samples at different time intervals. The reaction products were analyzed with a gas chromatograph equipped with a pulsed

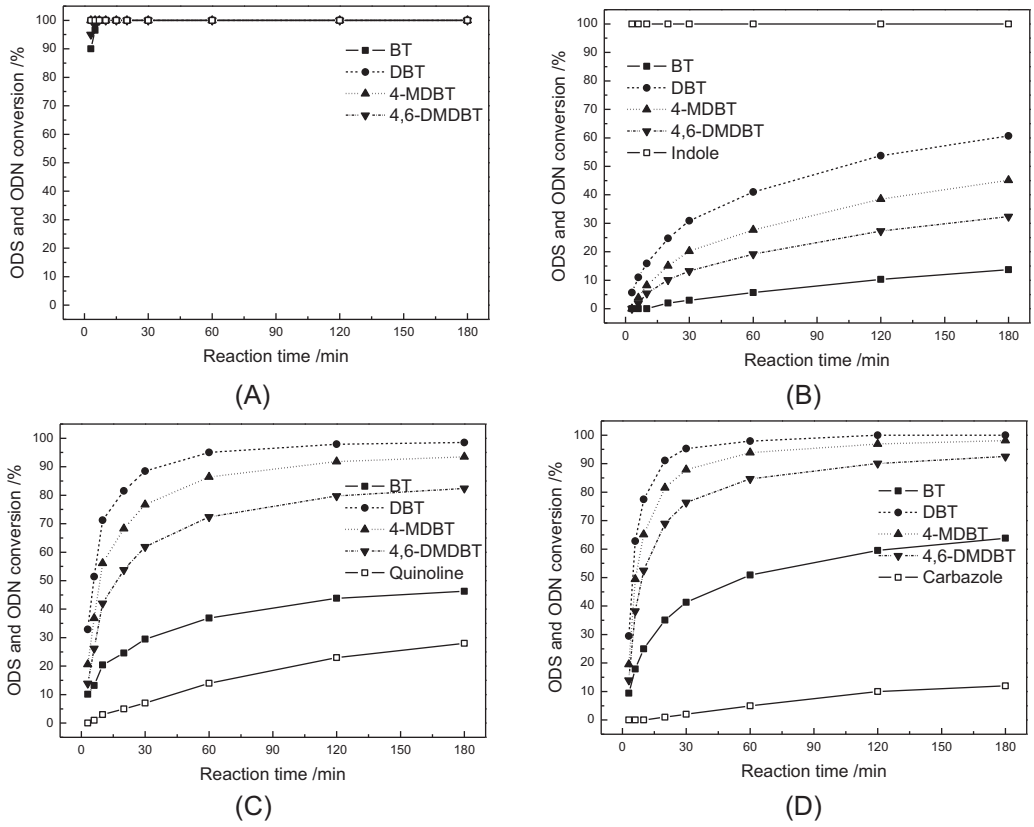

Fig. 1. Effect of nitrogen compounds on the ODS in a batch reactor: (A) Feed-M, (B) Feed-MI, (C) Feed-MQ, and (D) Feed-MC.

flame photometric detector (Agilent-6890-PFPD, HP-1, Cross linked methyl silicone gum, 25 m × 0.32 mm × 0.17 μm) to characterize the distribution of sulfur compounds between different classes. The operation of the PFPD detector was optimized using parameters (relationship between hydrogen (40 ml/min) and air (60 ml/min)) and temperature (1073 K) that were not exactly the same as those suggested by the manufacturer. In order to identify oxidation products of model reaction tests, GC–MS analyses were also performed using an Agilent 5973 mass selective detector coupled to the Agilent 6890 GC, operating in electron impact mode, equipped with an HP-1 capillary column (Cross linked methyl silicone gum, 25 m × 0.32 mm × 0.17 μm) using helium as the carrier gas. The oxidation conversion for ODS and ODN was defined as below:

$$\text{ODS conversion}\,(\%) = \frac{\text{moles of sulfur compounds reacted}}{\text{moles of sulfur compounds in feed}} \times 100$$

$$\text{ODN conversion}\,(\%) = \frac{\text{moles of nitrogen compounds reacted}}{\text{moles of nitrogen compounds in feed}} \times 100$$

3. Results and discussion

3.1. Effect of nitrogen compounds on the ODS

In order to examine the effects of various nitrogen compounds on the ODS, the activity tests were carried out for different model feed mixtures containing various nitrogen compounds. Fig. 1 shows the ODS conversion for the model feeds with indole (Feed-MI), quinoline (-MQ), and carbazole (-MC) as a function of reaction time. The ODS for the sulfur compounds was found to proceed promptly with complete conversion being reached within 5 min of reaction. In the presence of nitrogen compounds, however, the ODS activity was drastically decreased in the order: indole > quinoline > carbazole. The inhibition by indole was the most pronounced and significantly inhibited the ODS. Ishihara et al. studied ODS and ODN over MoO_3/Al_2O_3 catalyst and reported that the ODN inhibited the ODS with following the order: indole > quinoline > acridine > carbazole [20]. Caero et al. also found the oxidation of indole to oxindole over V_2O_5 catalysts, inhibiting the ODS of model sulfur compounds [33]. Jia et al. compared the effect of ODN reactivity of basic and non-basic nitrogen compounds on the ODS of thiophene and benzothiophene [34], which revealed that the ODS of thiophene was inhibited by basic nitrogen compound of pyridine, while the ODS of benzothiophene was inhibited by both basic and non-basic nitrogen compounds of pyridine or indole. These results suggested nitrogen compounds inhibited the ODS, which is attributed not only to competitive adsorption between sulfur and nitrogen compounds for catalytic sites, but also to their basic character.

In particular, for the sulfur compounds the ODS conversion was found to decrease in the order of DBT > 4-MDBT > 4,6-DMDBT > BT. It is known that the ODS is affected by electron density of sulfur atom in the compounds, following the order of 4,6-DMDBT (5.760) > 4-MDBT (5.759) > DBT (5.758) > BT (5.739) [22]. This implies that 4,6-DMDBT with higher electron density can be more easily oxidized to form corresponding sulfone. The ODS reactivity of 4,6-DMDBT was, however, found lower than that of DBT, suggesting that the methyl groups became an obstacle for the approach of the sulfur atom to the catalytic active phase, as also reported elsewhere [35].

A continuous fixed-bed reactor was also applied to examine the catalytic stability upon the introduction of indole, as shown in Fig. 2. It was observed that the more the indole was added, the greater the inhibition behavior was observed. As shown in Fig. 2(B), it can be seen that indole is preferentially converted prior to the ODS of sulfur compounds. These results suggest that nitrogen

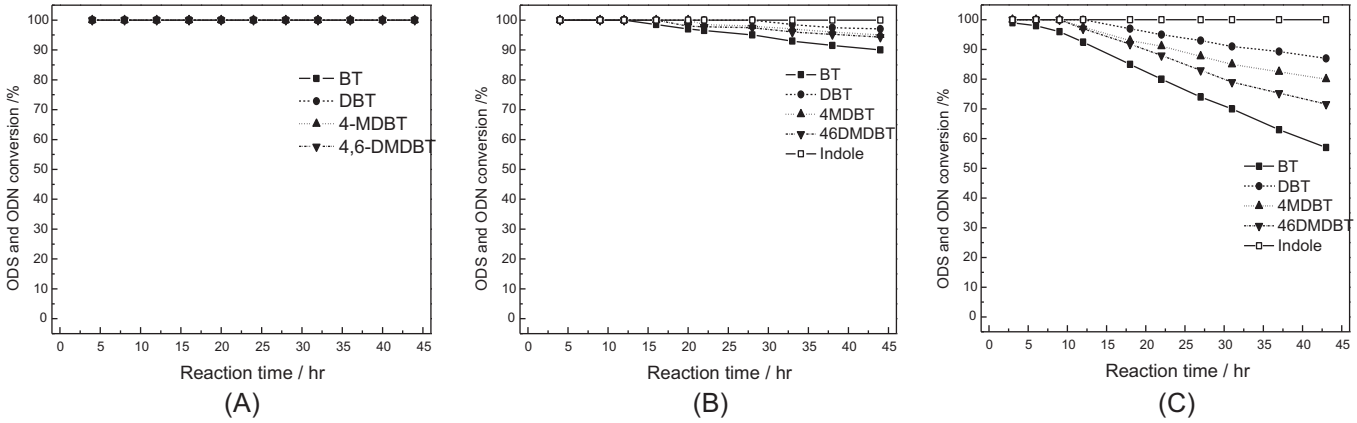

Fig. 2. Effect of N-compounds on the ODS in a flow reactor: (A) Feed-M, (B) Feed-MI 50 ppm N, and (C) Feed-MI 200 ppm N.

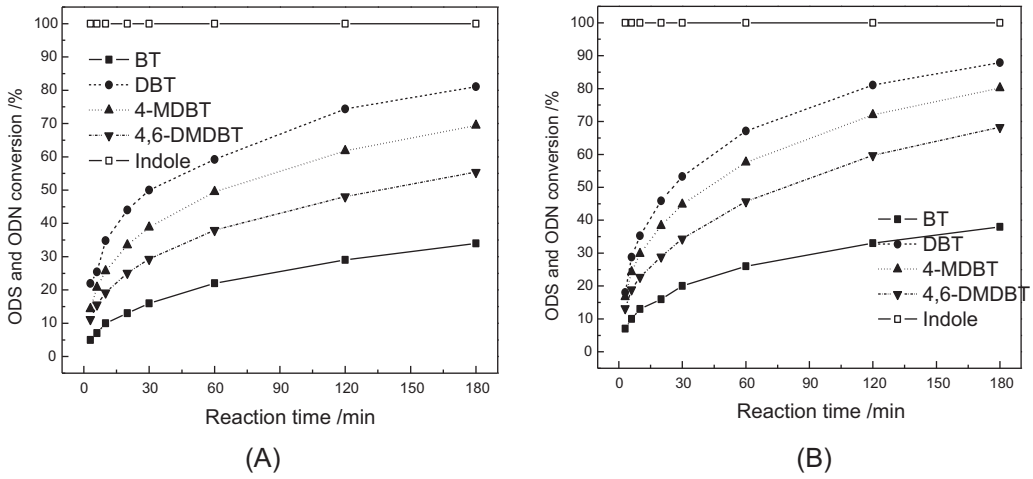

Fig. 3. Effect of 1-ring aromatic solvent (1Ar) on the ODS in a batch reactor: (A) Feed-M1AI 30% and (B) Feed-M1AI 70%.

compounds are competitive over the sulfur compounds in the oxidation, as indole has a higher reactivity than sulfur compounds in the oxidative reaction. Moreover, the oxidized reaction products might reside on the catalyst surface, blocking the adsorption sites where reactive oxygen species are formed. The amount of deposit on the catalyst surface was quantified by TGA measurements and compared as will be given in Fig. 7 .

3.2. Effect of aromatic solvents on the ODS

In order to examine the effect of aromatics solvents on the ODS, tetralin (1-ring aromatic solvent, 1Ar) or 1-methylnaphthalene (2-ring aromatic solvent, 2Ar) was added in the model feed oil (Feed-M), and their feed mixtures were denoted as Feed-M1A and Feed-M2A, respectively, as also summarized in Table 2. As shown in Fig. 3,

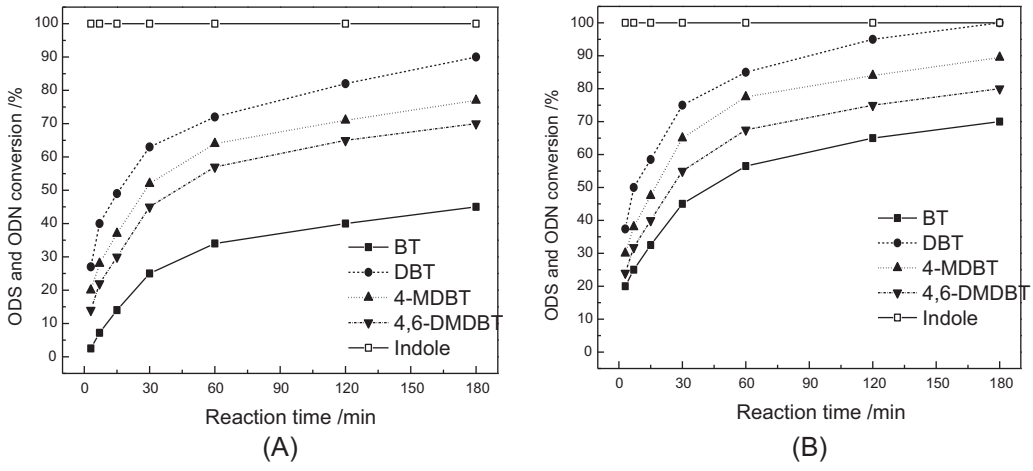

Fig. 4. Effect of 2-ring aromatic solvent (2Ar) on the ODS in a batch reactor: (A) Feed-M2AI 30% and (B) Feed-M2AI 70%.

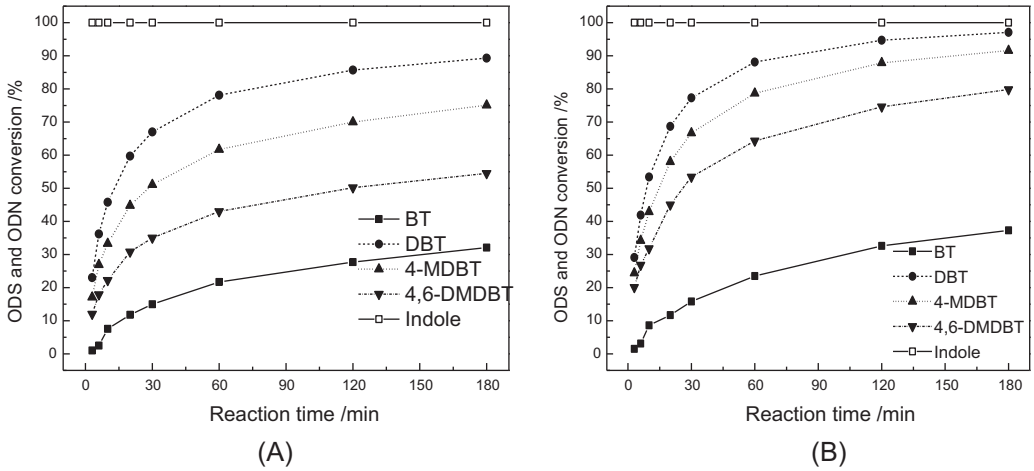

Fig. 5. Effect of aprotic solvent on the ODS in a batch reactor: (A) Feed-MAcI 30% and (B) Feed-MAcI 70%.

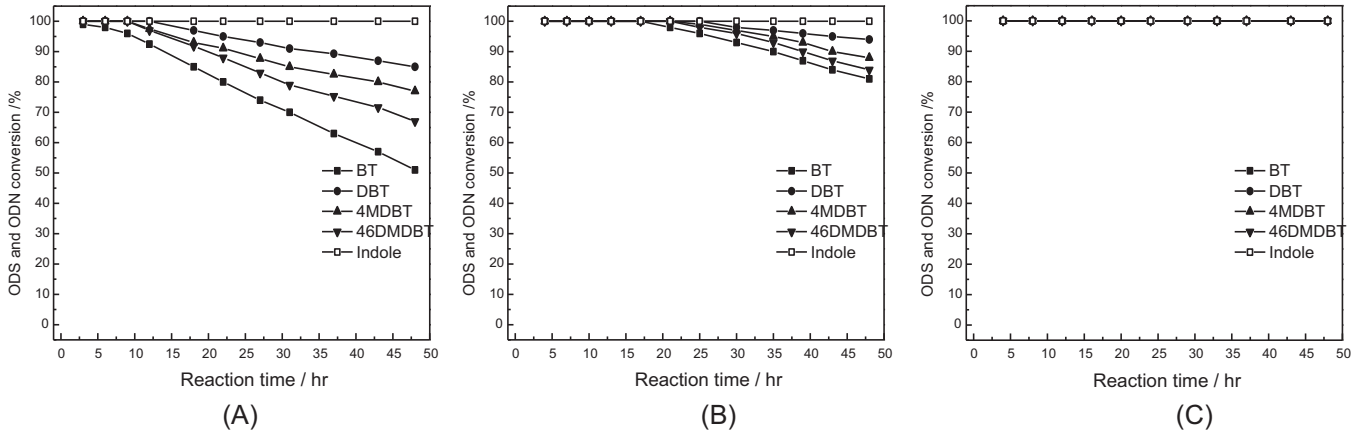

Fig. 6. Effect of aromatic and aprotic solvent on the ODS activities in a flow reactor: (A) Feed-MI 200 ppm, (B) Feed-M1AI 200 ppm, and (C) Feed-MAcI 200 ppm.

the ODS activity for sulfur compounds dissolved in aromatic solvent was slightly higher than that under aliphatic solvent (Fig. 1B). The increase in the aromatic solvent content from 30 to 70% led to a gradual increase in the ODS activity. Moreover, the addition of 2-ring aromatic solvent of 1-methylnaphthalene further enhanced the ODS conversion of sulfur compounds even with indole in the feed, as shown in Fig. 4, indicating that aromatics solvents play a beneficial role in reducing inhibition of oxidized S or N compounds.

3.3. *Effect of aprotic solvent on the ODS*

In order to investigate the effect of the aprotic solvent on the ODS, acetonitrile was employed as a model aprotic solvent in presence of indole. As shown in Fig. 5, the ODS activity was clearly increased upon the introduction of aprotic solvent. A continuous fixed-bed reactor was also applied to better investigate the catalytic performance and stability upon the introduction of aromatics and

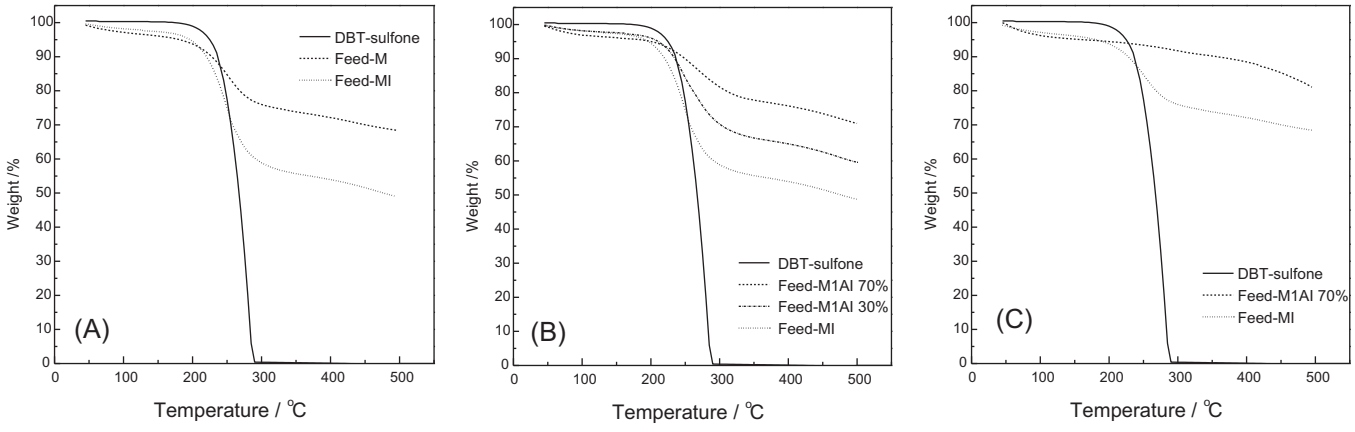

Fig. 7. TGA profiles Ti-SBA-15 catalysts collected after the ODS tests in batch reactor (A, B) and flow reactor (C).

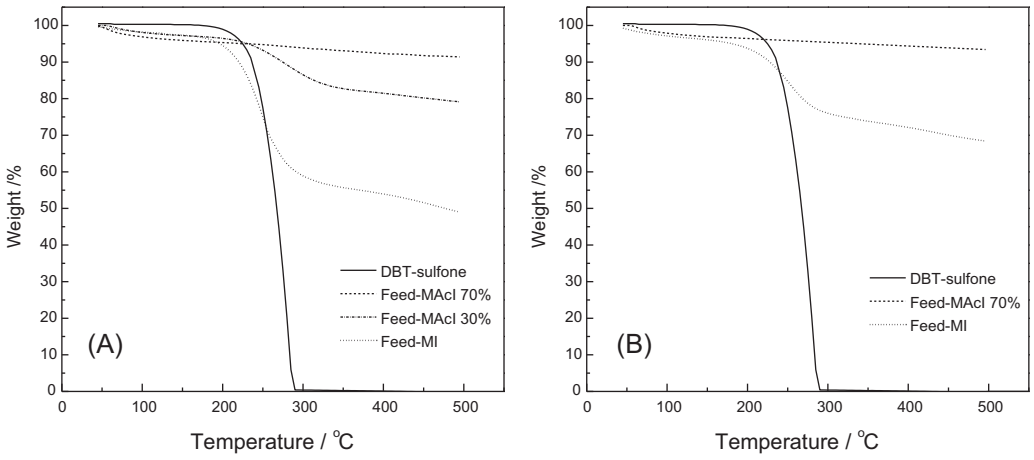

Fig. 8. TGA profiles Ti-SBA-15 catalysts collected after the ODS tests in the presence of solvents in batch reactor (A) and flow reactor (B).

aprotic solvent, as shown in Fig. 6. Comparing with the ODS without aromatics or aprotic solvent (Fig. 2), the addition of aromatics enhanced catalytic activity particularly at the early stage of reaction but with gradual deactivation with the progress of reaction being observed. In the case of using aprotic solvent, however, the ODS activity was maintained stable without deactivation for 48 h (Fig. 6C). Again, it was demonstrated that the addition of the solvents significantly improved the ODS activity in the presence of N compounds in feed oils.

3.4. Solubility of oxidized S and N products in aromatics or aprotic solvents

In order to verify the effect of the solvents, the solubility of the oxidized S or N products was measured in aliphatic, aromatic, and aprotic solvents. Generally, DBT is oxidized into DBTS and in the similar manner indole is converted to oxindole as a major product through the oxidation [20,32]. Table 3 summarizes the solubilities of DBTS, oxindole and isatin in the various solvents at 20 °C. For the organic solvents the solubilities of the oxidized compounds followed the order: acetonitrile > 1-methylnaphthalene > tetralin > tridecane. The oxidized compounds were nearly insoluble in tridecane, while they could well dissolve in aromatics and even better in aprotic solvents.

In order to confirm the solubility effects, the TGA measurements were conducted for the spent catalysts collected after the ODS of sulfur compounds with aromatic solvent in a batch reactor or a flow reactor as shown in Fig. 7. The TGA profile for the sample tested without aromatic solvent exhibited a weight loss of 40% in the temperature ranges of 200–300 °C due to the decomposition of the deposit of ODS products such as DBT-sulfone and 4,6-DMDBT-sulfone on the surface of the catalyst. However, in the presence of 1Ar, the weight loss of catalyst was reduced by 14%, indicating less deposit being formed on the catalyst. The TGA profiles of the spent catalysts that were collected after the ODS with addition of aprotic solvent in a batch reactor or in a continuous fixed-bed reactor are shown in Fig. 8. In the case of using aprotic solvent, the weight loss by the decomposition of the oxidized compounds was obviously reduced, indicating that the aprotic solvent could effectively dissolve the oxidized compounds to be readily desorbed from catalyst surface. In particular, the decomposition profile was rarely observed in the sample collected from the flow reactor. Thus,

Table 3
Solubilities of oxidized S and N compounds in various solvents at 20 °C.

Solvent	Solute($mg_{solute}\ g_{solvent}^{-1}$)		
	DBTS	Oxindole	Isatin
Tridecane	0.019	0.125	0.012
Tetralin	0.486	0.870	0.025
1-Methylnaphthalene	2.720	1.634	0.102
Acetonitrile	15.416	24.320	19.815

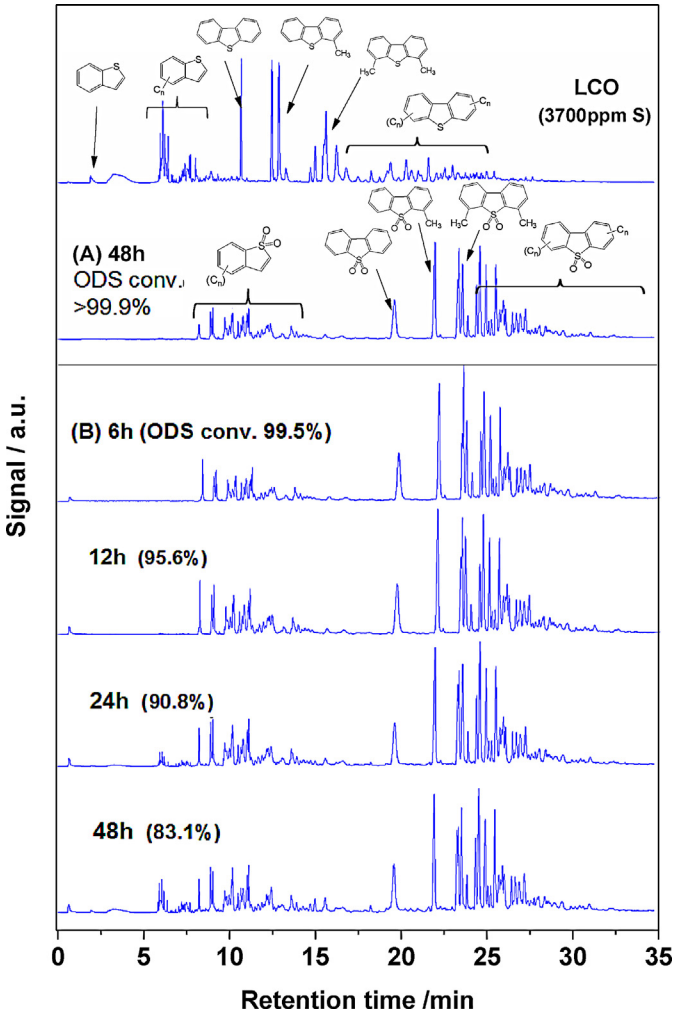

Fig. 9. GC-PFPD chromatograms of the ODS products of LCO in a flow reactor: (A) LCO + acetonitrile and (B) LCO only.

it was demonstrated that the addition of aprotic solvent in feed could maintain high and stable ODS activity for refractory sulfur and nitrogen compounds via minimizing the deposit of oxidized products on the catalyst surface.

3.5. Oxidative desulfurization of LCO

The ODS of real LCO feed was conducted in a flow reactor and samples were collected at different time intervals. Fig. 9 shows the GC-PFPD chromatograms of sulfur compounds present before and after the oxidation reaction of LCO. The identification of important reactants and products was made using standard samples. The sulfur compounds in the LCO feed are mostly alkyl-derivatives of BT and DBT. The GC peaks of S compounds in LCO shifted to higher retention times after 6 h of reaction time, implying that most of sulfur compounds in LCO were transformed to the corresponding sulfones. After 24 h of reaction, the GC peaks for unreacted alkyl-BT's became visible, indicating that the catalysts underwent gradual inhibition by the strong adsorption of reaction products such as oxidized S or N compounds on the surface of the active site of catalysts. However, in the case of using aprotic solvent mixed with LCO, the ODS activity was maintained active and stable with almost complete ODS conversion for 48 h of reaction, indicating the minimization of the product deposit on the catalyst surface. Therefore, it can be demonstrated that the addition of aprotic solvent in LCO feed could enhance the ODS activity and stability via dissolving the oxidized S and N products. In order to confirm the catalytic active phase and stability of the catalyst, Ti K-edge XANES spectroscopy was measured for fresh, spent, and calcined catalyst samples as shown in Fig. 10. The position and intensity of the pre-edge peak in the XANES spectrum is representing the transition of electrons from the 1s to the 3d level. The intensity of the pre-edge peak tends to increase in the order of octahedral, distorted octahedral, pentagonal, and, finally, tetrahedral coordination [38,39].

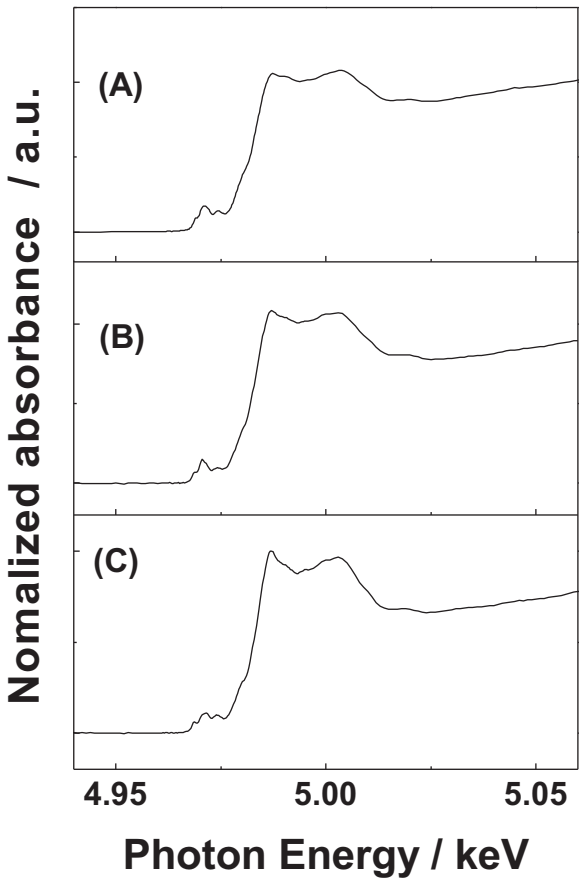

Fig. 10. Normalized XANES spectra of Ti-SBA-15 catalysts: (A) Ti-SBA-15 (fresh), (B) Ti-SBA-15 (spent, after LCO ODS), and (C) Ti-SBA-15 (spent and calcined at 400 °C)

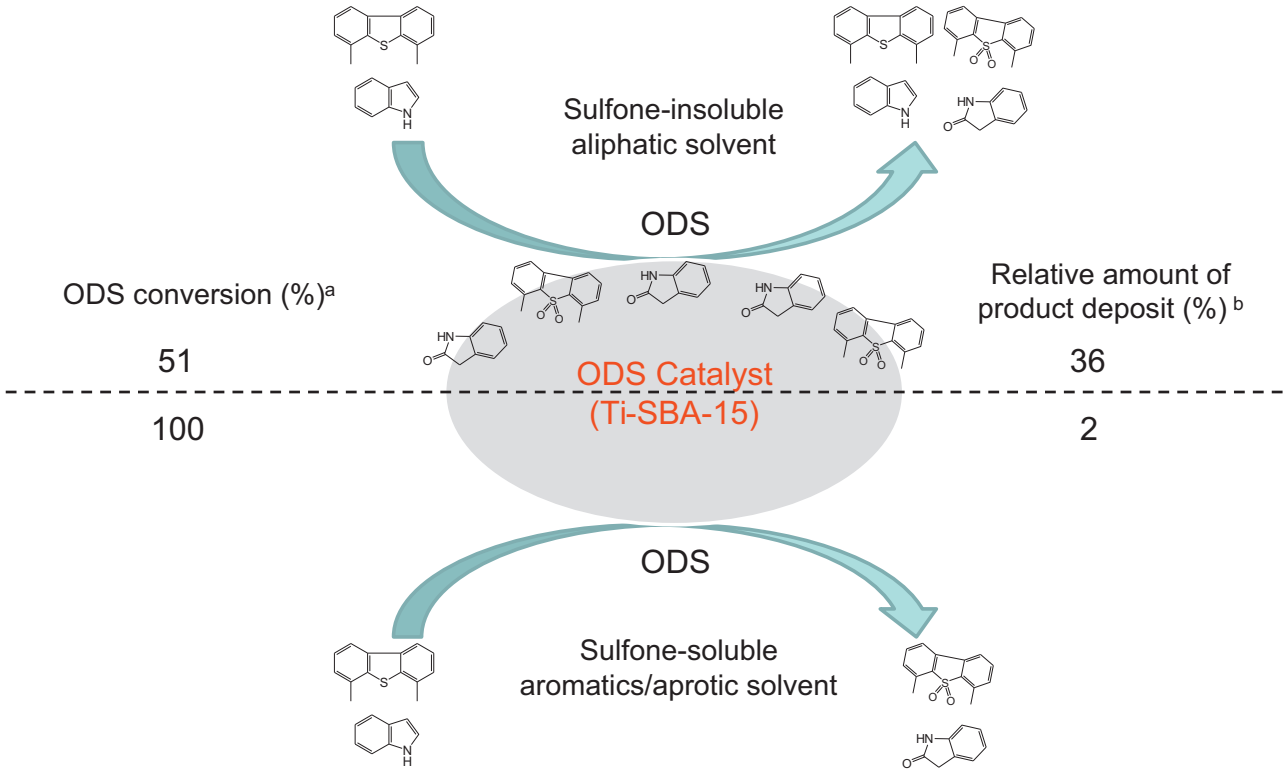

Fig. 11. Proposed reaction schematic of the ODS in the presence of nitrogen, aromatics and aprotic compounds. (a) Alkyl-BT ODS conversion at 48 h of reaction time in a flow reactor. (b) Estimated from TGA results for the ODS in a batch reactor

Table 4
Physical properties of Ti-SBA-15 samples.

Catalyst condition	Feed	BET surface area ($m^2\ g^{-1}$)	Pore volume ($cm^3\ g^{-1}$)	Ti content (wt%)
Fresh	–	764.6	1.08	5.0
Spent[a]	Feed-M	267.2	0.52	–
Spent[b]		598.2	0.93	4.8
Spent[a]	Feed-M1AI	313.1	0.60	–
Spent[a]	Feed-M2AI	467.6	0.72	–
Spent[a]	Feed-MAcI	574.8	0.89	–
Spent[a]	LCO	188	0.33	–
Spent[b]		568.8	0.87	4.7

[a] Dried at 120 °C.
[b] Calcined at 400 °C.

The XANES pre-edge peak intensity and position was not altered even after the ODS reaction and calcination. These results indicate that the Ti-catalysts remained stable during ODS reaction and regeneration.

The physical properties and Ti contents of the catalyst samples were also measured as listed in Table 4. The ODS of model S compounds and LCO led to a substantial loss in surface area and porosity of Ti-SBA-15 catalyst, indicating the deposit of oxidized S and N compounds on the catalysts. Instead, the catalysts after the ODS in aromatics solvent like tetralin (1Ar) or 1-methylnaphthalene (2Ar) gave rise to a partial recovery in the surface area and porosity. Moreover, the spent sample used in the aprotic solvent mixture (Feed-MAcI) gave only a little decrease in porosity, similarly to the case of calcined sample after the ODS, indicating the minimization of the ODS product deposit in the course of reaction. These results thus well support the beneficial role of aromatics or aprotic solvents on the ODS.

Overall, the ODS reaction schematic over Ti-SBA-15 catalyst in the presence of nitrogen, aromatic and aprotic compounds can be proposed as shown in Fig. 11. The refractory sulfur compounds are readily oxidized into sulfones on the Ti-SBA-15 catalyst in the absence of N compounds. In contrast, the presence of N compounds like indole drastically inhibits the ODS pathway due to its higher oxidative reactivity than S compounds and the strong interaction between the oxidized N compounds and the Ti-SBA-15 catalyst. It was, however, demonstrated that the addition of aromatic and aprotic solvents remarkably recovered the ODS activity, which was explained by the enhanced solubility of the oxidized S or N compounds in the aromatics and aprotic solvents.

4. Conclusions

The Ti-grafted SBA-15 catalyst showed high ODS activity for refractory sulfur compounds and LCO with using oxidizing agent of TBHP. In the presence of nitrogen compounds, the overall ODS activity was drastically decreased due to the competitive oxidation and the deposit of the oxidized S or N compounds on the catalyst surface, poisoning the adsorption sites where reactive oxygen species are formed. The addition of aromatic and aprotic solvent in feed oils recovered the ODS activity, which were attributed to the high solubility of the oxidized S or N compounds. Therefore, the presence of polycyclic aromatics compounds in LCO feed plays a beneficial role in the ODS reaction with minimizing the deposits of the oxidized products on the catalyst surface, maintaining good ODS reactivity. In particular, the addition of aprotic solvent in LCO could further enhance the ODS activity and stability.

References

[1] W.S. Zhu, H.M. Li, X. Jiang, Y.S. Yan, J.D. Lu, J.X. Xia, Energy and Fuels 21 (2007) 2514–2516.
[2] A. Stanislaus, A. Marafi, M.S. Rana, Catalysis Today 153 (2010) 1–68.
[3] L. Ding, Y. Zheng, Z. Zhang, Z. Ring, J. Cheng, Applied Catalysis A 319 (2007) 25–37.
[4] H. Yang, J. Chen, C. Fairbridge, Y. Briker, Y.J. Zhu, Z. Ring, Fuel Processing Technology 85 (2004) 1415–1429.
[5] H. Yang, J. Chen, Y. Briker, R. Szynkarczuk, Z. Ring, Catalysis Today 109 (2005) 16–23.
[6] T. Song, Z.S. Zhang, J.W. Chen, Z. Ring, H. Yang, Y. Zheng, Energy and Fuels 20 (2006) 2344–2349.
[7] I.V. Babich, J.A. Moulijn, Fuel 82 (2003) 607–631.
[8] H. Schulz, W. Böhringer, P. Waller, F. Ousmanov, Catalysis Today 49 (1999) 87–97.
[9] J.M. Manoli, P. Da Costa, F. Mauge, M. Brun, M. Vrinat, C. Potvin, Journal of Catalysis 221 (2004) 365–377.
[10] L. Lu, S. Cheng, J. Gao, G. Gao, M.Y. He, Energy and Fuels 21 (2007) 383–384.
[11] E. Gomez, V.E. Santos, A. Alcon, A.B. Martin, F. Garcia-Ochoa, Energy and Fuels 20 (2006) 1565–1571.
[12] A.N. Zhou, X.L. Ma, C. Song, Applied Catalysis B 87 (2009) 190–199.
[13] J. Zhang, A.J. Wang, X. Li, X.H. Ma, Journal of Catalysis 279 (2011) 269–275.
[14] C.P. Huang, B.H. Chen, J. Zhang, Z.C. Liu, Y.X. Li, Energy and Fuels 18 (2004) 1862–1864.
[15] F. Al-Shahrani, T. Xiao, S.A. Llewellyn, S. Barri, Z. Jiang, H. Shi, G. Martinie, M.L.H. Green, Applied Catalysis B 73 (2007) 311–316.
[16] A.D. Giuseppe, M. Crucianelli, F.D. Angelis, C. Crestini, R. Saladino, Applied Catalysis B 89 (2009) 239–245.
[17] G. Rodriguez-Gattorno, A. Galano, E. Torres-Garcia, Applied Catalysis B 92 (2009) 1–8.
[18] C. Jiang, J. Wang, S. Wang, H.Y. Guan, X. Wang, M. Huo, Applied Catalysis B 106 (2011) 343–349.
[19] D. Wang, E.W. Qian, H. Amano, K. Okata, A. Ishihara, T. Kabe, Applied Catalysis A 253 (2003) 91–99.
[20] A. Ishihara, D. Wang, F. Dumeignil, H. Amano, E.W. Qian, T. Kabe, Applied Catalysis A 279 (2005) 279–287.
[21] J.T. Sampanthar, H. Xiao, J. Dou, T.Y. Nah, X. Rong, W.P. Kwan, Applied Catalysis B 63 (2006) 85–93.
[22] S. Otsuki, T. Nonaka, N. Takashima, W. Qian, A. Ishihara, T. Imai, T. Kabe, Energy and Fuels 14 (2000) 1232–1239.
[23] J.M. Campos-Martin, M.C. Capel-Sanchez, J.L.G. Fierro, Green Chemistry 6 (2004) 557–562.
[24] G.-N. Yun, Y.-K. Lee, Fuel Processing Technology 114 (2013) 1–5.
[25] V.V.D.N. Prasad, K.E. Jeong, H.J. Chae, C.U. Kim, S.Y. Jeong, Catalysis Communications 9 (2008) 1966–1969.
[26] J.L. G-Gutierrez, G.A. Fuentes, M.E. H-Teran, F. Murrieta, J. Navarrete, F. J-Cruz, Applied Catalysis A 305 (2006) 15–20.
[27] A. Chica, A. Corma, M.E. Dómine, Journal of Catalysis 242 (2006) 299–308.
[28] A. Corma, M. Iglesia, F. Sanchez, Catalysis Letters 39 (1996) 153–156.
[29] L. Cedeno-Caero, M. Ramos-Luna, M. Mendez-Cruz, J. Ramirez-Solis, Catalysis Today 172 (2011) 189–194.
[30] T.W. Kim, M.J. Kim, F. Kleitz, M.M. Nair, R.G. Nicolas, K.E. Jeong, H.J. Chae, C.U. Kim, S.Y. Jeong, ChemCatChem 4 (2012) 687–697.
[31] F. Berube, S. Kaliaguine, Microporous and Mesoporous Materials 115 (2008) 469–479.
[32] P. Wu, T. Tatsumi, Chemistry of Materials 14 (2002) 1657–1664.
[33] L.C. Caero, J.F. Navarro, A. Gutierrez-Alejandre, Catalysis Today 116 (2006) 562–568.
[34] Y. Jia, G. Li, G. Ning, C. Jin, Catalysis Today 140 (2009) 192–196.
[35] J. Qiu, G. Wang, D. Zeng, Y. Tang, M. Wang, Y. Li, Fuel Processing Technology 90 (2009) 1538–1542.
[36] A. Bianconi, E. Fritsch, G. Calas, J. Petiau, Physical Review B 32 (6) (1985) 4292–4295.
[37] G.C. Laredo, S. Leyva, R. Alvarez, M.T. Mares, J. Castillo, J.L. Cano, Fuel 81 (2002) 1341–1350.
[38] M.D. Corbett, B.R. Chipko, Biochemical Journal 183 (2) (1979) 269–276.
[39] G.A. Waychunas, American Mineralogist 72 (1987) 89–101.